

Development of a Europium Nanoparticles Lateral Flow Immunoassay for NGAL Detection in Urine and Diagnosis of Acute Kidney Injury

Moli Yin

Jilin Medical University

Yuanwang Nie

Jilin Medical University

Hao Liu

Jilin Medical University

Lei Liu

Jilin Medical University

Lu Tang

Jilin Medical University

Yuan Dong

Jilin Medical University

Chuanmin Hu

Jilin Medical University

Huiyan Wang (✉ jlmpcwhy@163.com)

Jilin Medical University

Research Article

Keywords: neutrophil gelatinase-associated lipocalin (NGAL), monoclonal antibody, lateral flow immunoassay, acute kidney injury (AKI)

Posted Date: March 22nd, 2021

DOI: <https://doi.org/10.21203/rs.3.rs-331019/v1>

License:  This work is licensed under a Creative Commons Attribution 4.0 International License.

[Read Full License](#)

Version of Record: A version of this preprint was published at BMC Nephrology on January 14th, 2022.
See the published version at <https://doi.org/10.1186/s12882-021-02493-w>.

Development of a europium nanoparticles lateral flow immunoassay for NGAL detection in urine and diagnosis of acute kidney injury

Moli Yin¹, Yuanwang Nie², Hao Liu², Lei Liu¹, Lu Tang¹, Yuan Dong², Chuanmin Hu¹, Huiyan Wang^{1,*}

¹Jilin Collaborative Innovation Center for Antibody Engineering, Jilin Medical University, Jilin, Jilin 132013, PR China

²Academy of laboratory, Jilin Medical University, Jilin, Jilin 132013, PR China

* Author for correspondence: jlmpcwhy@163.com

1 **Abstract**

2 **Background:**AKI is related to severe adverse outcomes and mortality with
3 Coronavirus Infection Disease 2019 (COVID-19) patients, that early diagnosed and
4 intervened is imperative. Neutrophil gelatinase-associated lipocalin (NGAL) is one of
5 the most promising biomarkers for detection of acute kidney injury (AKI), but current
6 detection methods are inadequacy, so more rapid, convenient and accuracy methods
7 are needed to detect NGAL for early diagnosis of AKI. Herein, we established a rapid,
8 reliable and accuracy lateral flow immunoassay based on europium nanoparticles
9 (Eu-NPS-LFIA) for the detection of NGAL in human urine specimens.

10 **Methods:**A double-antibody sandwich immunofluorescent assay using europium
11 doped nanoparticles was employed and the NGAL monoclonal antibodies conjugate
12 as labels were generated by optimizing electric fusion parameters. Eighty-three urine
13 samples were used to evaluate the clinical application efficiency of this method.

14 **Results:**The quantitative detection range of NGAL in AKI was 1-3000 ng/mL, and
15 the detection sensitization was 0.36 ng/mL. The CV of intra-assay and inter-assay
16 were 2.57%-4.98% and 4.11%-7.83%, respectively. Meanwhile, the correlation
17 coefficient between Eu-NPS-LFIA and ARCHITECT analyzer was significant
18 ($R^2=0.9829$, $n=83$, $p<0.01$).

19 **Conclusions:**Thus, a faster and easier operation quantitative assay of NGAL for AKI
20 has been established, which is very important and meaningful to diagnose the early
21 AKI, suggesting that the assay can provide an early warning of final outcome of
22 disease.

23 **Keywords:** neutrophil gelatinase-associated lipocalin (NGAL), monoclonal antibody,
24 lateral flow immunoassay, acute kidney injury (AKI)

25 **Background**

26 Coronavirus Infection Disease 2019 (COVID-19) has widely spread in the worldwide
27 scale with serious disaster[1].Acute kidney injury (AKI) has a higher rate of
28 morbidity and mortality in common complication for critical illnesses and counted
29 about 5%-7% of hospitalized patients in world[2].Several studies have evaluated the
30 development of AKI is more strongly related to worse outcomes and mortality rates of
31 COVID-19, described incidence of AKI that ranges widely from 0.5 to 36.6% in
32 COVID-19 patients[3].Early detection and precise treatments of AKI can implement
33 better preventive strategies and prevent deterioration of renal function and renal
34 failure, effectively contain progression of the COVID-19 hospitalized patients[4].
35 Current diagnosis of AKI is confirmed by the concentration of serum creatinine (SCr),
36 which is steady unless at least 50% of damaged kidney function[5]. Thus, several
37 novel biomarkers were developed to improve the diagnostic specificity in early stages
38 of AKI[6]. Among them, neutrophil gelatinase-associated lipocalin (NGAL) has been
39 recognized as one of the promising biomarkers candidate for detection of AKI. NGAL
40 is a 25 kDa glycoprotein associated with gelatinase from neutrophil and usually exist
41 at lower level in human tissues such as stomach, colon and kidney, but its expression
42 is dramatically increased in serum and urine when the kidney was with ischemic or
43 nephrotoxic injury[7]. In AKI, several studies have discovered NGAL concentration
44 in urine is significantly associated with SCr concentration[8]. In recent years, various
45 electrochemical and immunological methods have been developed for the detection of
46 NGAL, instance of electrochemical determination, solid-phase proximity ligation
47 assay and enzyme-free electrochemical immunoassay[9, 10]. However, these
48 techniques require precise equipment, specialized personnel and professional
49 interpretation of the results. Therefore, to develop an effective and convenient
50 detection assay for NGAL concentration in the urine is critical for this disorder
51 monitoring.

52 Lateral flow immunoassays (LFIA) has been regard as desired screening assays on
53 account of simplicity, in-situ analysis and easy to work[11]. The LFIA with
54 fluorescent microparticles have already been used for detection of various microbial
55 pathogens and several inflammation markers[12, 13]. Due to urine contain low
56 viscosity and low content of solids so that it would be highly compatible with the LF
57 platform, hence urine has been successfully examined in analysis of pregnancy tests,
58 Schistosoma antigens and albumin[14]. The high sensitivity nanoparticles labeled in
59 LFIA as fluorescent probes has been continually researched over past decades, gold
60 nanoparticles are the most widely used, but the application of the lateral flow tests
61 based on traditional labels is limitedfor there poor identification and weaker the
62 signal[15]. Several novel nanoparticles have been generally applied to improve the
63 sensitivity of LFIA, including carbon nanoparticles, quantum dots, fluorescent dyes,
64 magnetic nanolabels and europium (III) dye-doped nanoparticles[16]. The fluorescent
65 EU-NPS (III) as carriers can improve 100-fold sensitivity contrast with colloidal gold
66 nanoparticles labeled in LFIA[17]. EU-NPS with long fluorescence lifetimes, strong
67 stability, high precision and not disturb the sample quality, have used in
68 sandwich-type immunoassays of medical diagnostics recently[18]. Currently there are
69 antibodies available for the development of NGAL have been applied to different
70 platforms for NGAL detection, but not available in LFIA based on EU-NPS labels
71 experimented on the detection of NGAL in addition to UCP technology-based lateral
72 flow assay [19, 20].

73 Here, we established a new method with EU-NPS as labels of LFIA for the rapid,
74 sensitive and early measurement of NGAL in urine based on two mAbs 1G1 and 2F4
75 which are discovered by our lab.The method is double-antibody sandwich
76 immunofluorescent assay using europium doped nanoparticles and NGAL
77 monoclonal antibody conjugate as labels. The mAb 1G1 was conjugated with
78 fluorescent nanoparticles and the mAb 2F4 was used to capture EU-NPS-1G1-antigen
79 complex in T-line. Our results showed that EU-NPS-LFIA could be used for the early
80 NGAL detection in urine and allow improvement in the treatment of SARS-CoV-2
81 patients.

82

83 **Methods**

84 **Urine samples**

85 The total of 83 Human urine samples were harvested from Affiliated Hospital of Jilin
86 Medical University. These samples were stored at -80°C. The ethical guidelines were
87 strictly complied in the experiment, was provided by the Affiliated Hospital of Jilin
88 Medical University. All subjects were received informed consent for the study of
89 urine samples.

90

91 **Expression and purification of NGAL**

92 The human NGAL gene sequence from Genbank (NP_005555.2) was synthesized by
93 BGI Genomics and added restriction enzymes *Hind*III and *Xho*I at both ends. The
94 plasmids were digested with *Hind*III and *Xho*I, and then cloned into the pSecTag2A
95 vector. The constructed plasmids were sequenced to confirm without mutation, and
96 then transformed into CHO cells by the LipofectamineTM2000. After 8 days, the cell
97 supernatant was collected after filtering 0.45μm filter. The expressed NGAL-6×His
98 protein was purified with the Ni-NTA column, and the different fractions were
99 collected and appraised by sodium dodecyl sulfate-polyacrylamide gel electrophoresis
100 (SDS-PAGE) . The BCA Protein Quantification Kit measured the concentration of
101 protein.

102 The purified recombinant protein was subjected in 12% SDS-PAGE, then adsorbed
103 onto a polyvinylidene fluoride (PVDF) membrane. After the membrane was blocked
104 in tris buffer with 1% Tween-20 (TBST) solution containing 5% skimmed milk at RT
105 for 2 h, incubated with HRP-conjugated anti-6×His tag antibody (1:5000) in the dark
106 for 1 h at RT, visualized with Benzidine after washed with TBST and visualized by
107 Bio-Rad Western blotting detection system (DNR Bio-Imaging Systems Ltd., Israel).

108

109 **Generation and purification of Monoclonal antibodies**

110 In the first immunization, the female BALB/c mice (age of 6 weeks, a total of 10)
111 were immunized with 50μg NGAL-6×His recombinant protein emulsified in equal

112 dosage of complete Freund's adjuvant, and accessional immunized were
113 accomplished with protein emulsified in incomplete Freund's adjuvant. Two
114 hypodermic injections on the back of mice and subsequent were intraperitoneal
115 injections spaced 21 days. The serum samples were collected one week after the third
116 injection, and the titre of antiserum was determined with indirect enzyme-linked
117 immunosorbent assay (ELISA)[21]. Three days before fusion, mice were performed
118 to booster immunization with 50 μ g of NGAL-6 \times His diluted with 0.9% NaCl.

119 The isolated immune mice spleen cells and the SP2/0 myeloma cells mixed at a
120 ratio of 3:1 to fuse in a platinum electrode LF498-3 fusion chamber (BEX Co., Ltd,
121 Japan) as described literature[22]. Briefly, the mixed cell was washed twice with 10
122 mL electrofusion buffer (0.3 M mannitol, 0.1 mM CaCl₂, 0.1 mM MgCl₂, pH 7.2),
123 re-suspended at a concentration of 2 \times 10⁷ cells/mL. The fusion was completed using
124 an alternating current voltage of 50 V at 0.8 MHz for 20 s, direct current pulse voltage
125 of 450 V of 2 repetitions for 0.5 s, and post-fusion was 50 V at 0.8 MHz for 7 s.
126 Finally, the electric-treated cell suspension was moved from the fusion chamber into
127 4.5 mL of preheated RPMI 1640 (20% fetal bovine serum) for 30 min at 37°C, then
128 cultured in 96-well plates and incubated with 5% CO₂ at 37°C. After 24 h,
129 hypoxanthine-aminopterin-thymidine (HAT) was supplemented to each well. The Cell
130 culture supernatants were screened by ELISA after 9 days fusion, and calculated
131 number of hybridoma clones. The BALB/c mice which injected with paraffin oil in
132 advance were inoculated with 1 \times 10⁶ of NGAL hybridoma cells, the ascites were
133 purified by Protein A column.

134

135 **Identification of monoclonal antibodies**

136 The immunoglobulin subclasses of antibodies were analyzed using the antibody
137 subclass identification kit. The indirect ELISA screened the specific monoclonal
138 antibodies (MAbs) by using purified recombinant NGAL-6 \times His protein and
139 PCT-6 \times His protein. The interaction between antigen and antibodies were determined
140 with BIACore T200 system (GE Healthcare, Stockholm, Sweden) in HBS-EP buffer
141 (0.005% surfactant P20, 10 mM Hepes, pH 7.4, 3 mM EDTA, 150 mM NaCl). The

142 NGAL antigen was adsorbed on CM5 biosensor chips reaching 400-480 response
143 units (RU) by an amine coupling kit. The antibodies (2F4 and 1G1) were diluted in
144 HBS-EP buffer were slowly passed over the chip with 50 µL/min for 5 min,
145 respectively, and subsequently HBS-EP buffer injected over the chip to monitor the
146 dissociation phase for 4 min. The sensor chips were regenerated with Glycine solution
147 (pH 3.0) following the dissociation phase. For each analyte passed over the chip, the
148 specific responses from the antigen flow channel could subtract non-specific
149 responses for the control flow channel. The fitted saturation binding curves were
150 plotted based on concentrations of analyte for equilibrium binding responses to
151 calculate KD.

152 The specificity of anti-NGAL monoclonal antibodies was determined by Western
153 Blot. Briefly, the NGAL proteins were done to 12% SDS-PAGE, then adsorbed onto
154 polyvinylidene fluoride (PVDF) membrane that activated by soaking in methanol for
155 15 s, and then subjected to the electrophoresis conditions in 100 V for 2 h. After
156 blocking in Tris-HCl buffer with 1% Tween-20 solution (TBST) containing 5%
157 skimmed milk at RT for 2 h, the membrane was incubated with mouse anti-NGAL
158 mAb as the primary antibodies at 4°C. The next day, membrane was washed with
159 TBST and incubated with anti-mouse conjugated HRP IgG in the dark for 1.5 hour at
160 RT. Finally, the membrane was visualized by the Western blot detection system of
161 enhanced chemiluminescence (ECL).

162

163 **Conjugation of Europium nanoparticles**

164 The Anti-NGAL monoclonal antibody 1G1 were covalently conjugated to EU-NPS
165 with standard procedure of Bangs Laboratories. Briefly, 100 µL EU-NPS were added
166 to 900 µL 0.05 M MES (pH 7.0) and dispersed by ultrasound, vibrated for 15 min at
167 RT in the presence of 0.08 M N-hydroxysulfosuccinimide (NHS) and 0.05 M
168 carbodiimide (EDC).The activated EU-NPS ware washed with coupling buffer (0.05
169 mM H₃BO₃, 0.04 mM Na₂B₄O₇, pH 7.5) and reacted with 0.3 mg antibody for 2.5 h at
170 RT. The europium-conjugated compound was incubated in 1000 µL blocking buffer
171 (10% BSA, 20% tween-20, 0.05 M Tris-HCl) for 1h, added to 1000 µL stock

172 solutions (10% BSA, 20% trehalose, 20% tween-20, 0.05 M Tris-HCl) to store at
173 4°C.

174

175 **The development of LFIA**

176 The Lateral flow immunochromatography strips were consisted of nitrocellulose
177 membrane, conjugate pad, sample pad and absorbing pad. The glass fiber membranes
178 were soaked in the blocking buffer (20% trehalose, 10% BSA, 20% tween-20, 0.05 M
179 Tris, 3.2 mM EDTA.Na₂, pH 8.6) for 1.5 h. The concentration of 1 mg/mL mAb 2F4
180 was coated on the test line (TL) of nitrocellulose membrane, and goat-anti-mouse IgG
181 1 mg/mL was coated on the same NC membrane at a distance of 4 mm to form a
182 quality control line (CL), the spray volume of dispenser instrument was set at 1
183 µL/cm. The membrane and glass fiber mat were dried for 48 h at 45°C before tested.
184 The 2 µL EU-NPS-1G1 conjugate particles were coated on the conjugate pad, and
185 fluorescence signal was measured by immunofluorescent analyzer (Guangzhou
186 Labsim Biotech Co., Ltd).

187

188 **Clinical sample testing and analysis**

189 The serial concentrations of NGAL standards antigen (10, 50, 100, 200, 400, 800,
190 1500, 2000 and 3000 ng/mL) were prepared by using FBS to strengthen specific
191 reaction of bioconjugate, each concentration done three replicates. After the clinical
192 samples were added onto the sample pads, the results of fluorescence intensity on the
193 T line (HT) and the C line (HC) were recorded by the reader. Quantitative detection
194 was completed by the HT/HC ratio to effectively eliminate strips (T and C) difference
195 and matrsample standard matrix effects[23]. The standard curve was plotted against
196 each concentration of NGAL and HT/HC ratio.

197

198 **Statistical analysis**

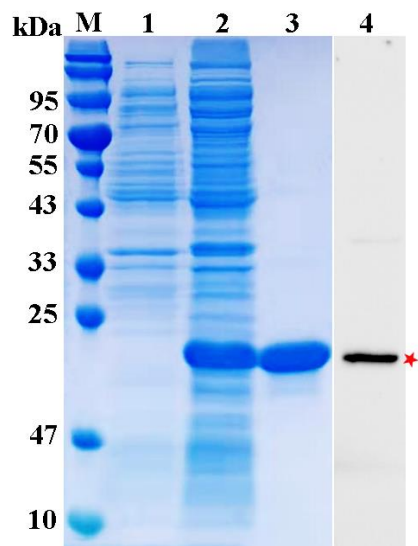
199 The Passing-Bablok regression analysis and Bland-Altman plot were performed by
200 analysis of variance (ANOVA) of MedCalc and SPSS 17.0 software. All data were
201 showed as mean value with standard deviation (mean ± S.D.).

202

203 **Results**

204 **Expression and purification of recombinant NGAL protein**

205 The pSecTag2A-NGAL recombinant plasmid was transfected into CHO cells. The
206 NGAL-6×His protein mainly expressed in cell supernatant and subsequently purified
207 by Ni Sepharose. The purified recombinant NGAL protein was obtained about 95%
208 purity and analyzed by SDS-PAGE with molecular approximate weight of 23.7 kDa .
209 Western blot also confirmed the recombinant protein NGAL expression and
210 purification (Figure 1).



211

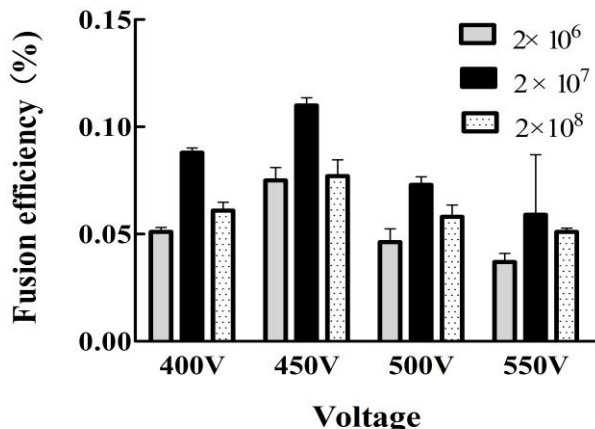
212 **Figure 1. Expression and purification of NGAL-6xHis.** (A) Purification of
213 NGAL-6xHis protein were appraised by SDS-PAGE and Western blot, Lane M,
214 protein marker; Lane 1, supernatant of CHO cell culture; Lane 2, supernatant of
215 induced sample; Lane 3, purified protein ; Lane 4, Western blot analysis of
216 NGAL-6xHis expression.

217

218 **Generation of monoclonal antibodies**

219 First, we compared the effects of DC voltage on cell membrane perforation under
220 different electric field intensities, and the pulse amplitude was 400 V, 450 V, 500 V
221 and 550 V respectively, so as to optimize the electric fusion scheme. According to
222 previous reports, cell concentration has a significant impact on fusion efficiency[24].

223 The mixed suspension of isolated spleen cells and SP2/0 myeloma cells was
224 transferred into the fusion chamber at different concentrations of approximately 2×10^6 ,
225 2×10^7 , and 2×10^8 cells /mL. The fusion efficiency was the highest at 450 V DC, and
226 the optimal cell concentration was 2×10^7 cells/mL (Figure 2).



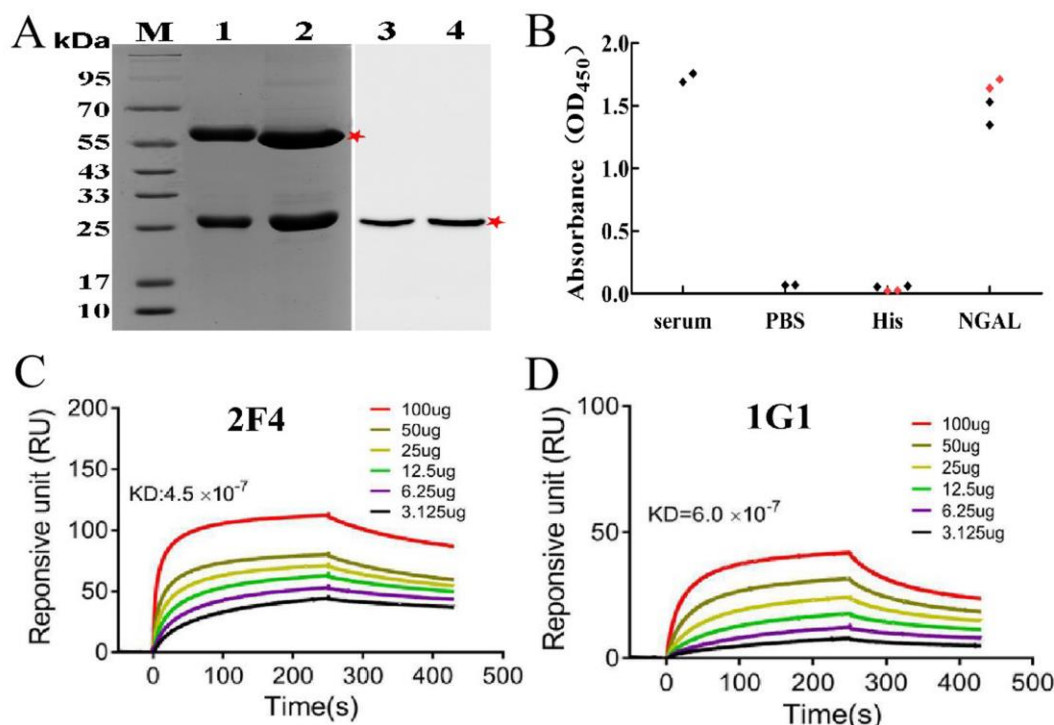
227
228 **Figure 2. Comparison of fusion efficiency using different the puncture pulse**
229 **height.** The fusion cells were seeded into 96-well plates at approximately 2×10^5
230 cells/well. A total of 480 wells was assessed for each condition. The calculated
231 method of the fusion efficiency (%): the total number of colonies in 480 wells were
232 counted,then divided by the number of input B cells and multiplied by 100. The
233 columns represent the average fusion efficiency (%) of 3 experiments, the error bars
234 represent the SD.

235

236 Characterization of monoclonal antibodies

237 The mAbs were purified by Protein A column. The purified mAbs were separated by
238 12% SDS-PAGE, two bands with molecular weight 55 kDa and 25 kDa were
239 observed. Western blot indicated that all monoclonal antibodies specifically bind to
240 human NGAL protein (Figure 3A). After cell electrofusion and sub-cloning, the
241 supernatants of hybridomas were detected by indirect ELISA with NGAL-6×His and
242 PCT-6×His to ensure antibodies specific binding to the NGAL. Two highly positive
243 hybridomas (1G1, 2F4) with specific NGAL binding while without cross-reaction to
244 PCT-6×His were successfully selected for production and purification of mAbs
245 (Figure 3B). To detect the affinity of two monoclonal antibodies, the interaction
246 between antibodies with different concentrations and NGAL protein was analyzed by
247 BIACore T200 system. The kinetic diagram showed that the affinity of 2F4 and 1G1

248 were 4.5×10^{-7} and 6.0×10^{-7} , respectively (Figure 3C and 3D). The isotypes of those
 249 two mAbs which were detected by commercial kits were IgG1.



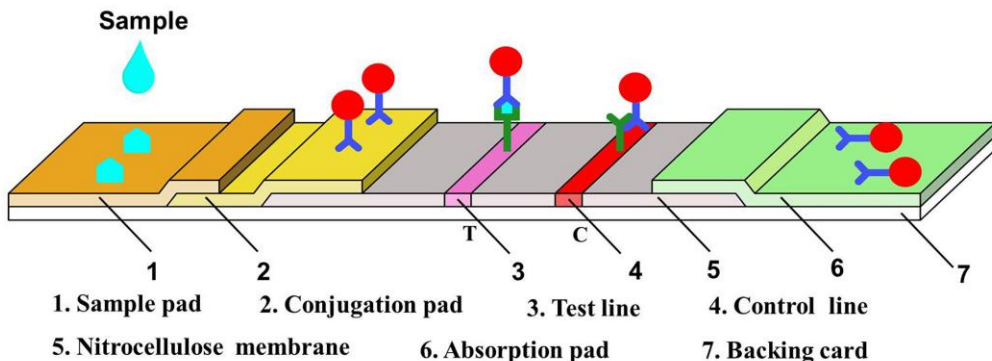
250
 251 **Figure 3. Characterization of monoclonal antibodies.** (A) The ascites were
 252 assessed by SDS-PAGE and Western blot, Lane M, protein marker; Lane 1, purified
 253 the ascites of 2F4; Lane 2, purified the ascites of 1G1; Lane 3, Western blot analysis
 254 of mAb 2F4 ; Lane 4, Western blot analysis of mAb 1G1. (B) The Cross-reactivity of
 255 2 hybridoma lines was tested by Indirect ELISA, NGAL-6×His and PCT-6×His were
 256 coated onto microtiter plates. The positive control was a NGAL-6×His immune serum;
 257 PBS were used as blank control. (C) Relative affinity of MAb 2F4. (D) Relative
 258 affinity of MAb 1G1.

259

260 EU-NPS-LFIA Procedures

261 Based on EU-NPS as labels and the sandwich-type immunoassay, the lateral flow
 262 immunoassay was established for detection of NGAL. As schematically illustrated
 263 (Figure 4), TL and CL of nitrocellulose membrane were coated with the monoclonal
 264 antibodies 2F4 and goat anti-mouse IgG EU-NPS-1G1 was labeled on the conjugate
 265 pad. The sample containing NGAL antigen migrated towards the conjugate pad to
 266 combine with EU-NPS-1G1 and form antigen-antibody complexes. Subsequently, the
 267 complexes were captured by mAb 2F4 in T-line while migrating to form sandwich
 268 complexes. Excess complex was combined the goat anti-mouse IgG. Test strips were

269 measured with a fluorescence detector after 15 min.



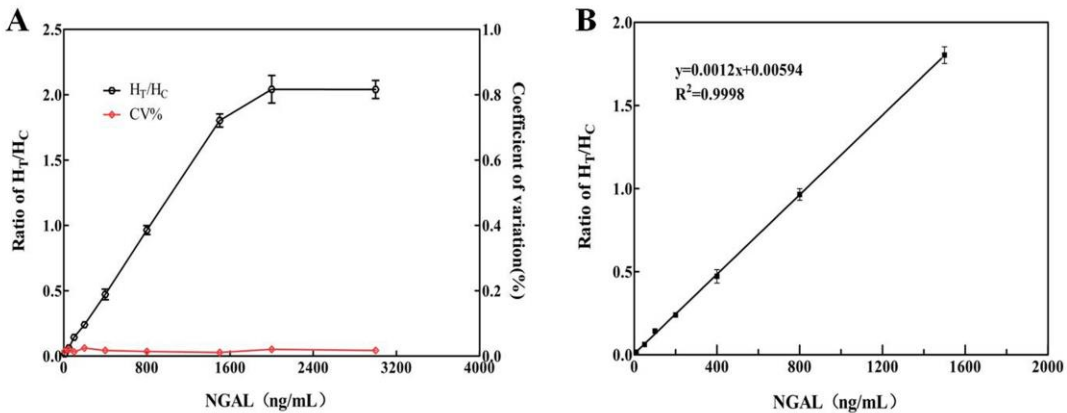
270

271 **Figure 4.** Schematic description of fluorescence immunoassay system employed
272 Europium-conjugated NGAL mAbs.

273

274 **Performance evaluation**

275 The antibody pairs (2F4- labeled1G1) as detector and capture antibodies were used to
276 establish fluorescent immunochromatographic, and the analytical performances of
277 EU-NPS-LFIA was evaluated by building the standard curve. The relative
278 fluorescence intensity ratio(HT/HC) was increased with NGAL concentration.
279 EU-NPS-1G1 showed reaction to mAb 2F4 (Figure 5A). The high-dose hook
280 influence wasn't detected when concentration of antigen reached 3000 ng/mL. The
281 regression equation was exhibited as follows: $y = 0.0012 x + 0.0059$ ($R^2=0.99$), where
282 y represents the ratio of HT/HC , x represents the concentrations of NGAL (Figure
283 5B).The detection limit (LOD) was 0.36 ng/mL (3 times the standard deviation of the
284 blank, n = 20) calculated by the Clinical Laboratory Standards Institute (CLSI)
285 Guideline EP17-A2, the NGAL concentration had linear relationship in the range of
286 1-1500 ng/mL[25].



287

288 **Figure 5. Standard curves for NGAL.** (A) The ratio of HT/HC, by antibody pairing
 289 in LFIA, the antibody pairs 2F4-labeled1G1 ratio of HT/HC rose with increasing
 290 concentration of NGAL. (B) The standard curve of NGAL.

291

292 Precision

293 Recovery experiments of the intra-assay and inter-assay were performed to evaluate
 294 precision and reproducibility of immunological method. The different concentrations
 295 (50, 200 and 800 ng/mL) of NGAL standard substance were added to negative urine
 296 samples. The intra-assay precision was calculated with three replicates at each spiked
 297 concentration in 1 day, and inter-assay precision was calculated with three replicates
 298 at each spiked concentration at every three days for fifteen days continuously[26].
 299 The results were shown in **Table 1**, the calculated intra-assay CV ranged from 2.57%
 300 to 4.98% (n=10), lower than 10%. The inter-assay CV ranged from 4.11% to 7.83%
 301 (n=15), lower than 10% too. These results explained that the precision of the
 302 developed LFIA was a high level, and reproducibility was an acceptable level.

303 **Table 1. Reproducibility analysis of the EU-NPS-LFIA test strip by intra-assay
 304 and inter-assay precision**

NGAL (ng/mL)	Intra-Assay Precision (n = 10)		Inter-Assay Precision (n = 15)	
	Mean±SD (ng/mL)	CV (%)	Mean±SD (ng/mL)	CV (%)
50	49.57±0.003	4.98	51.28±0.037	5.68
200	199.18±0.009	3.84	202.78±0.019	7.83
800	799.76±0.025	2.57	801.68±0.039	4.11

305

306

307 Specificity

308 The specificity of the test strips was evaluated by adding endogenous substances in
309 normal and different concentrations urine samples, including creatinine, glucose and
310 urea nitrogen. As shown in **Table 2**, the results indicated that all relative deviations
311 (RD) was in the range of $\pm 10\%$, suggesting antigen-antibody interaction were stable
312 and illustrating the specificity of test strips was acceptable toward NGAL.

313 **Table 2. The specificity study of the EU-NPS-LFIA with different interfering
314 endogenous substances**

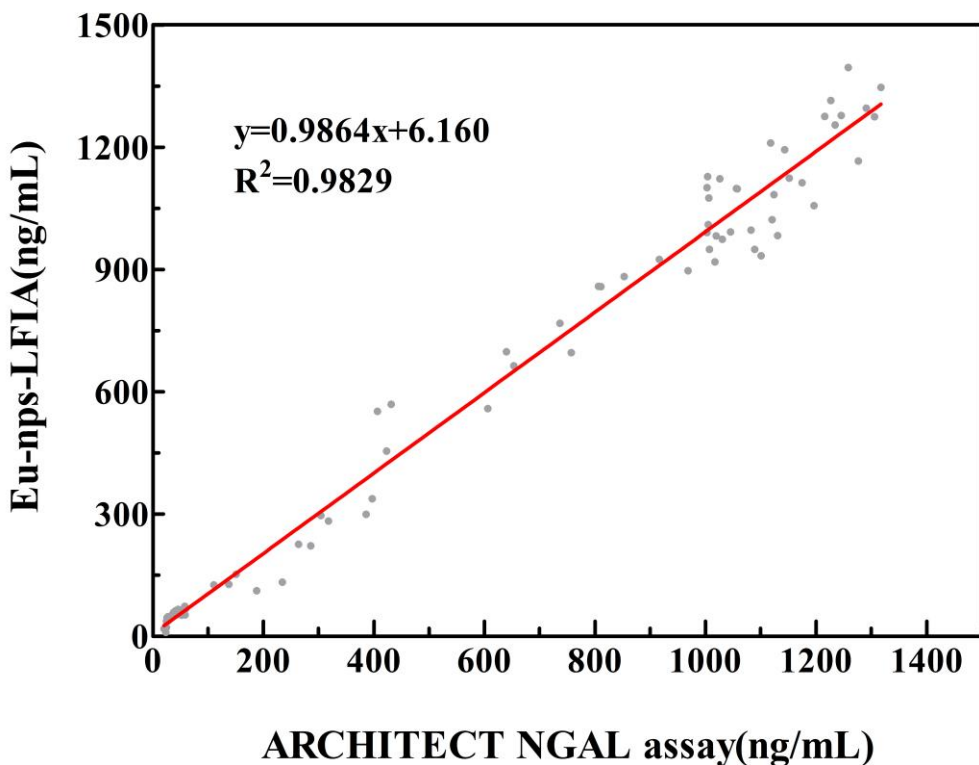
Interfering Substance	NGAL (27.64ng/mL)		NGAL (53.72ng/mL)	
	Value	RD (%)	Value	RD (%)
control	0.037 \pm 0.002	0.54	0.069 \pm 0.003	2.35
Creatinine(10 mg/mL)	0.035 \pm 0.008	-4.55	0.067 \pm 0.009	-2.06
glucose(10 mg/mL)	0.036 \pm 0.007	-2.55	0.071 \pm 0.006	3.83
urea nitrogen(100 mg/mL)	0.036 \pm 0.004	2.72	0.064 \pm 0.008	-5.98

315 Note: RD = (Value-Standard value) / Standard value.

316

317 **Clinical samples tests**

318 In order to appraise applicative competence of the NGAL based on EU-NPS-LFIA for
319 determination of clinical samples, a total of 83 urine samples containing 26 low value
320 samples (11-70 ng/mL), 19 median value samples (110-800 ng/mL), 38 high value
321 samples (800-1740 ng/mL), were measured on the ARCHITECT urine NGAL assay.
322 The results of correlation coefficient (R^2) of the regression curve was 0.9829 ($p<0.01$),
323 indicating that the two detection methods had a significant linear relationship (where
324 x represents concentrations of NGAL obtained by the ARCHITECT analyzer, y
325 represents values measured by developed test strips) (Figure 6). Thus, the developed
326 EU-NPS-LFIA for determination of NGAL was very accurate in clinical testing.



327
328 **Figure 6. Comparison of EU-NPS-LFIA with ARCHITECT urine assay**
329 **estimated correlation of the results for NGAL clinical test.**

331 Discussion

332 The sensitivity europium-based lateral fluorescence immunoassays (EU-NPS-LFIA)
333 for detection of NGAL in human urine and diagnosis of acute kidney injury during the
334 COVID-19 pandemic has been developed in our study. AKI developed in 89% of
335 severe patients with COVID-19, and a majority of patients had predominantly oliguria
336 when appears earlier than plasma Creatinine[27]. Biomarkers increased elevated
337 levels at admission, which associated with increased mortality. NGAL is one of these
338 biomarkers, levels of which may positive correlation with risk for mortality in
339 COVID-19 hospitalized patients[28]. The low efficiency of PEG fusion in
340 conventional methods to causes difficulties in obtaining functional antibodies, we
341 optimized electric fusion parameters that enabled enhancement of fusion efficiency to
342 prepare of viable hybridomas, and obtained two anti-NGAL mAbs, one conjugated
343 with EU-NPS while the other used as capture antibodies[24].

344 In recent years, many studies have been reported to develop several NGAL rapid
345 diagnostic immunoassays, including the photoelectrochemical immunosensor and
346 three electrochemical immunosensors, the solid-phase proximity ligation assay and
347 lateral flow assay[29]. In one study, immunosensor has been made by NGAL capture
348 antibodies immobilized to screen-printed-modified carbon electrode and labeled
349 addition of secondary antibody against NGA to PB-NP-decorated g-C₃N₄ nanosheets
350 forming a sandwich on the SPCE[10]. The other study developed antibody against
351 NGAL was immobilized on a screen printed electrode (SPCE) modified with
352 electropolymerized aniline deposited on top of an electrosprayed
353 graphene/poly-aniline (G/PANI)[29]. Two reports showed the LOD varied widely
354 from 0.6 pg/mL to 21.1 ng/mL, depending on the g-C₃N₄ nanosheets with N element
355 enhanced electrocatalytic efficiency of the nanohybrids than graphene nanosheets, and
356 the LOD of the NGAL assay varies depending on immunosensor, conjugated-complex
357 and antibodies[30]. According to those studies, we enlightened that sensitivity of
358 LFIA could be improved by basing on different fluorescence nanoparticles mentioned
359 in the preamble section.

360 Fluorescence immunoassays have advantage in various detection fields, especially
361 in mature quantum dots, that sensitivity was influenced by the monoclonal antibodies
362 and fluorescent materials, and could greatly improve by EU-NPS and specific
363 monoclonal antibodies to use the fluorescent probes[31]. The europium nanoparticles
364 were applied to fluorescence lateral flow immunoassay strips had matured in the
365 detection field, and enhanced several advantages of LFIA for assay sensitivity,
366 specificity and stability[32]. Due to excellent properties of the EU-NPS that the limit
367 of detection for NGAL in this method was 0.36 ng/mL, while the mean urine NGAL
368 levels was about 7.0 ng/mL in healthy individuals[33]. The developments and
369 application about the EU-NPS-LFIA of NGAL are still in initial phase, this assay need
370 to test NGAL of serum samples with COVID- 19 patients for which improvement in
371 the treatment in the future of works.

372

373 **Conclusions**

374 In the study, we successfully got two mouse anti-NGAL mAbs (2F4, 1G1) and were
375 labeled with EU-NPS to establish the lateral flow immune technique. The
376 EU-NPS-LFIA was found to detect NGAL in a wide range of 1-3000 ng/mL within
377 15 min, the detection sensitivity reached 0.36 ng/mL. These anti-NGAL mAbs could
378 be reliability utilized in fluorescence lateral flow immunoassay of NGAL detection in
379 the urine samples, so that it should be applicable in the AKI diagnosis.

380

381 **Abbreviations**

382 COVID-19: Coronavirus Infection Disease 2019; AKI: Acute kidney injury; SCr: serum creatinine;
383 NGAL: neutrophil gelatinase-associated lipocalin; LFIA: Lateral flow immunoassays; EU-NPS (III):
384 europium (III) dye-doped nanoparticles; ELISA: enzyme-linked immunosorbent assay; MAbs:
385 monoclonal antibodies

386 **Acknowledgements**

387 Not applicable.

388 **Authors' contributions**

389 HYW designed the experiments; MLY, YWN, HL and LL performed study planning, data analysis,
390 manuscript drafting and manuscript review.LT, YD and CMH revised the manuscript.All authors gave
391 intellectual input to the manuscript and approved final version.

392

393 **Funding**

394 The authors disclosed receipt of the following financial support for the research, authorship, and/or
395 publication of this article:This work was supported by the ‘Research and Development of Industrial
396 Technology’ Program of Jilin Province, PR China (grant nos. 20180623045TC and 20170204005YY),
397 National Natural Science Foundation of China (no. 21827812) and National Training Program of
398 Innovation and Entrepreneurship for Undergraduates (nos. 201913706017 and 202013706002).

399 **Availability of data and materials**

400 The datasets used and/or analyzed during the current study are available from the corresponding author
401 on reasonable request

402 **Ethics approval and consent to participate**

403 The study was performed on the basis of institutional ethical guidelines, approved by the Affiliated

404 hospital of Jilin Medical University in China. All procedures were followed the principles Declaration
405 of Helsinki, informed consent was obtained from all subjects.

406 **Consent for publication**

407 Not applicable.

408 **Competing interests**

409 The authors declare that they have no conflict of interest.

410 **Author details**

411 ¹Jilin Collaborative Innovation Center for Antibody Engineering, Jilin Medical University, Jilin, Jilin
412 132013, PR China. ²Academy of laboratory, Jilin Medical University, Jilin, Jilin 132013, PR China.

413 **References**

- 415 1. Zheng X, Zhao Y, Yang L: **Acute Kidney Injury in COVID-19: The Chinese Experience.** *Seminars in nephrology* 2020, **40**(5):430-442.
- 416 2. Mandelbaum T, Scott D, Lee J, Mark R, Malhotra A, Waikar S, Howell M, Talmor D: **Outcome of critically ill patients with acute kidney injury using the Acute Kidney Injury**
417 **Network criteria.** *Critical care medicine* 2011, **39**(12):2659-2664.
- 418 3. Al-Hwiesh A, Mohammed A, Elnokeety M, Al-Hwiesh A, Al-Audah N, Esam S,
419 Abdul-Rahman I: **Successfully treating three patients with acute kidney injury secondary**
420 **to COVID-19 by peritoneal dialysis: Case report and literature review.** *Peritoneal dialysis*
421 **international** 2020, **40**(5):496-498.
- 422 4. Shabaka A, Rovirosa-Bigot S, Guerrero Márquez C, Alonso Riaño M, Fernández-Juárez G:
423 **Acute kidney injury and nephrotic syndrome secondary to COVID-19-associated focal**
424 **segmental glomerulosclerosis.** *Nefrologia* 2021.
- 425 5. Shapiro N, Trzeciak S, Hollander J, Birkhahn R, Otero R, Osborn T, Moretti E, Nguyen H,
426 Gunnerson K, Milzman D *et al:* **The diagnostic accuracy of plasma neutrophil**
427 **gelatinase-associated lipocalin in the prediction of acute kidney injury in emergency**
428 **department patients with suspected sepsis.** *Annals of emergency medicine* 2010,
429 **56**(1):52-59.e51.
- 430 6. Alge J, Arthur J: **Biomarkers of AKI: a review of mechanistic relevance and potential**
431 **therapeutic implications.** *Clinical journal of the American Society of Nephrology* 2015,
432 **10**(1):147-155.
- 433 7. Gabbard W, Milbrandt E, Kellum J: **NGAL: an emerging tool for predicting severity of**
434 **AKI is easily detected by a clinical assay.** *Critical care* 2010, **14**(4):318.
- 435 8. Wagener G, Jan M, Kim M, Mori K, Barasch J, Sladen R, Lee H: **Association between**
436 **increases in urinary neutrophil gelatinase-associated lipocalin and acute renal**
437 **dysfunction after adult cardiac surgery.** *Anesthesiology* 2006, **105**(3):485-491.
- 438 9. Kannan P, Tiong H, Kim D: **Highly sensitive electrochemical determination of neutrophil**
439 **gelatinase-associated lipocalin for acute kidney injury.** *Biosensors*
440 **bioelectronics** 2012, **31**(1):32-36.

- 443 10. Zhang F, Zhong H, Lin Y, Chen M, Wang Q, Lin Y, Huang: **A nanohybrid composed of**
444 **Prussian Blue and graphitic CN nanosheets as the signal-generating tag in an**
445 **enzyme-free electrochemical immunoassay for the neutrophil gelatinase-associated**
446 **lipocalin.** *Mikrochimica acta* 2018, **185**(7):327.
- 447 11. Zuk R, Ginsberg V, Houts T, Rabbie J, Merrick H, Ullman E, Fischer M, Sizto C, Stiso S,
448 Litman D: **Enzyme immunochromatography--a quantitative immunoassay requiring no**
449 **instrumentation.** *Clinical chemistry* 1985, **31**(7):1144-1150.
- 450 12. Juntunen E, Myyryläinen T, Salminen T, Soukka T, Pettersson K: **Performance of fluorescent**
451 **europtium(III) nanoparticles and colloidal gold reporters in lateral flow bioaffinity assay.**
452 *Analytical biochemistry* 2012, **428**(1):31-38.
- 453 13. Swanson C, D'Andrea A: **Lateral flow assay with near-infrared dye for multiplex**
454 **detection.** *Clinical chemistry* 2013, **59**(4):641-648.
- 455 14. Juntunen E, Arppe R, Kalliomäki L, Salminen T, Talha S, Myyryläinen T, Soukka T,
456 Pettersson K: **Effects of blood sample anticoagulants on lateral flow assays using**
457 **luminescent photon-upconverting and Eu(III) nanoparticle reporters.** *Analytical*
458 *biochemistry* 2016, **492**:13-20.
- 459 15. Chen A, Yang S: **Replacing antibodies with aptamers in lateral flow immunoassay.**
460 *Biosensors bioelectronics* 2015, **71**:230-242.
- 461 16. Chen Y, Fu Q, Xie J, Wang H, Tang Y: **Development of a high sensitivity quantum**
462 **dot-based fluorescent quenching lateral flow assay for the detection of zearalenone.**
463 *Analytical bioanalytical chemistry* 2019, **411**(10):2169-2175.
- 464 17. Zhang F, Zou M, Chen Y, Li J, Wang Y, Qi X, Xue Q: **Lanthanide-labeled**
465 **immunochromatographic strips for the rapid detection of Pantoea stewartii subsp.**
466 **stewartii.** *Biosensors bioelectronics* 2014, **51**:29-35.
- 467 18. Nankoberanyi S, Mbogo G, LeClair N, Conrad M, Tumwebaze P, Tukwasibwe S, Kamya M,
468 Tappero J, Nsobya S, Rosenthal P: **Validation of the ligase detection reaction fluorescent**
469 **microsphere assay for the detection of Plasmodium falciparum resistance mediating**
470 **polymorphisms in Uganda.** *Malaria journal* 2014, **13**:95.
- 471 19. Li H, Mu Y, Yan J, Cui D, Ou W, Wan Y, Liu S: **Label-free photoelectrochemical**
472 **immunosensor for neutrophil gelatinase-associated lipocalin based on the use of**
473 **nanobodies.** *Analytical chemistry* 2015, **87**(3):2007-2015.
- 474 20. Lei L, Zhu J, Xia G, Feng H, Zhang H, Han Y: **A rapid and user-friendly assay to detect the**
475 **Neutrophil gelatinase-associated lipocalin (NGAL) using up-converting nanoparticles.**
476 *Talanta* 2017, **162**:339-344.
- 477 21. Xu H, Dong Y, Guo J, Jiang X, Liu J, Xu S, Wang H: **Monoclonal antibody production and**
478 **the development of an indirect competitive enzyme-linked immunosorbent assay for**
479 **screening T-2 toxin in milk.** *Toxicon* 2018, **156**:1-6.
- 480 22. Kato M, Sasamori E, Chiba T, Hanyu Y: **Cell activation by CpG ODN leads to improved**
481 **electrofusion in hybridoma production.** *Journal of immunological methods* 2011,
482 **373**:102-110.
- 483 23. Huang X, Aguilar Z, Xu H, Lai W, Xiong Y: **Membrane-based lateral flow**
484 **immunochromatographic strip with nanoparticles as reporters for detection: A review.**
485 *Biosensors bioelectronics* 2016, **75**:166-180.

- 486 24. Weeratna R, Comanita L, Davis H: **CPG ODN allows lower dose of antigen against**
487 **hepatitis B surface antigen in BALB/c mice.** *Immunology cell biology* 2003, **81**(1):59-62.
- 488 25. Tong Q, Chen B, Zhang R, Zuo C: **Standardization of clinical enzyme analysis using frozen**
489 **human serum pools with values assigned by the International Federation of Clinical**
490 **Chemistry and Laboratory Medicine reference measurement procedures.** *Scandinavian*
491 *journal of clinical laboratory investigation* 2018, **78**:74-80.
- 492 26. Huang D, Ying H, Jiang D, Liu F, Tian Y, Du C, Zhang L, Pu X: **Rapid and sensitive**
493 **detection of interleukin-6 in serum via time-resolved lateral flow immunoassay.**
494 *Analytical biochemistry* 2020, **588**:113468.
- 495 27. Luther T, Bülow-Anderberg S, Larsson A, Rubertsson S, Lipcsey M, Frithiof R, Hultström M:
496 **COVID-19 patients in intensive care develop predominantly oliguric acute kidney**
497 **injury.** *Acta anaesthesiologica Scandinavica* 2021, **65**(3):364-372.
- 498 28. Abers M, Delmonte O, Ricotta E, Fintzi J, Fink D, de Jesus A, Zaremba K, Alehashemi S,
499 Oikonomou V, Desai J: **An immune-based biomarker signature is associated with**
500 **mortality in COVID-19 patients.** *JCI insight* 2021, **6**(1).
- 501 29. Yukird J, Wongtangprasert T, Rangkupan R, Chailapakul O, Pisitkul T, Rodthongkum N:
502 **Label-free immunosensor based on graphene/polyaniline nanocomposite for neutrophil**
503 **gelatinase-associated lipocalin detection.** *Biosensors bioelectronics* 2017, **87**:249-255.
- 504 30. Gong Y, Li M, Wang Y: **Carbon nitride in energy conversion and storage: recent advances**
505 **and future prospects.** *ChemSusChem* 2015, **8**(6):931-946.
- 506 31. Yeo S, Bao D, Seo G, Bui C, Kim D, Anh N, Tien T, Linh N, Sohn H, Chong C *et al*:
507 **Improvement of a rapid diagnostic application of monoclonal antibodies against avian**
508 **influenza H7 subtype virus using Europium nanoparticles.** *Scientific reports* 2017,
509 **7**(1):7933.
- 510 32. Chen E, Xu Y, Ma B, Cui H, Sun C, Zhang M: **MonascusCarboxyl-Functionalized,**
511 **Europium Nanoparticle-Based Fluorescent Immunochromatographic Assay for Sensitive**
512 **Detection of Citrinin in Fermented Food.** *Toxins* 2019, **11**(10).
- 513 33. Bolignano D, Coppolino G, Campo S, Aloisi C, Nicocia G, Frisina N, Buemi M: **Neutrophil**
514 **gelatinase-associated lipocalin in patients with autosomal-dominant polycystic kidney**
515 **disease.** *American journal of nephrology* 2007, **27**(4):373-378.

Figures

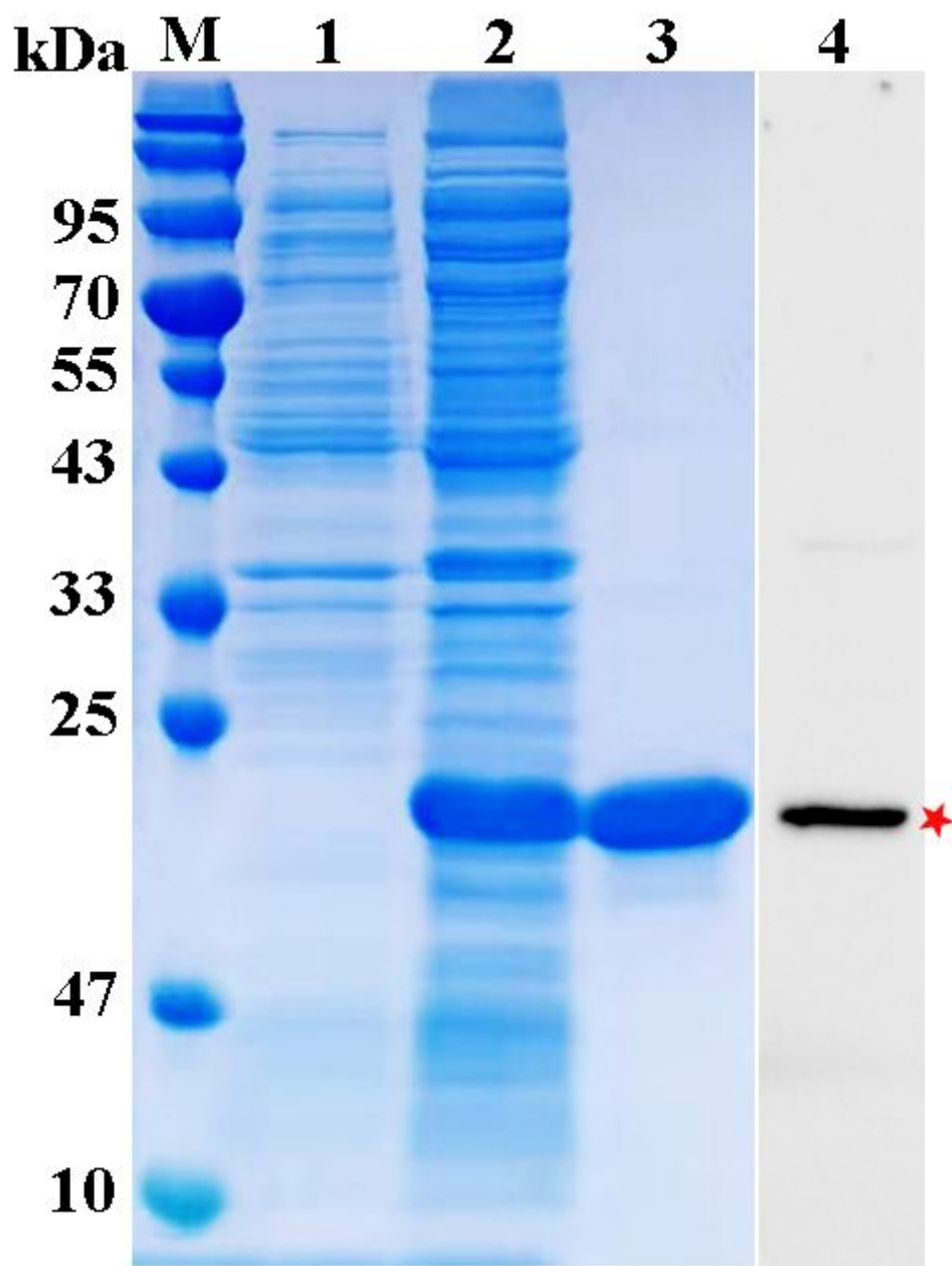


Figure 1

Expression and purification of NGAL-6×His. (A) Purification of NGAL-6×His protein were appraised by SDS-PAGE and Western blot, Lane M, protein marker; Lane 1, supernatant of CHO cell culture; Lane 2, supernatant of induced sample; Lane 3, purified protein ; Lane 4, Western blot analysis of NGAL-6×His expression.

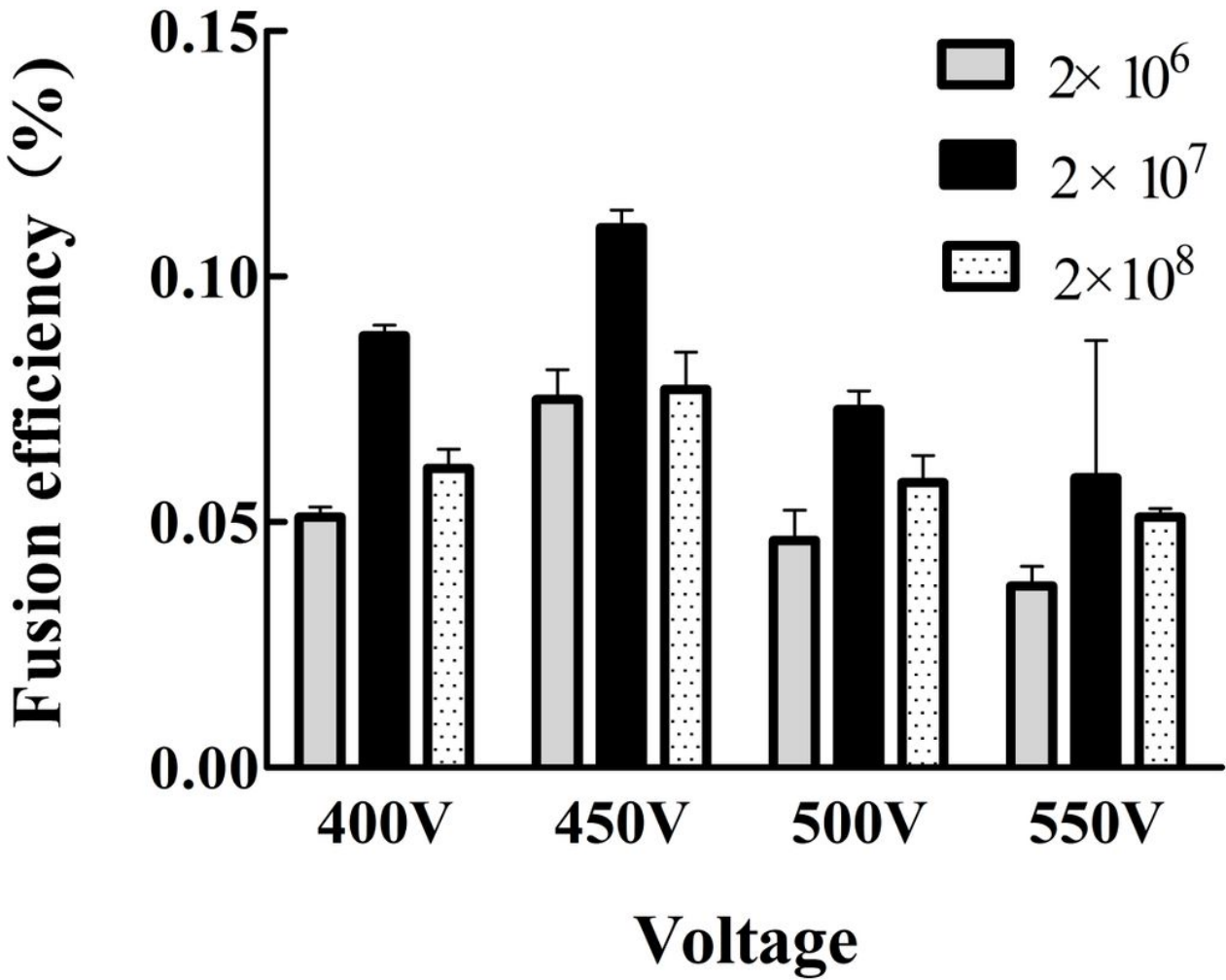


Figure 2

Comparison of fusion efficiency using different the puncture pulse height. The fusion cells were seeded into 96-well plates at approximately 2×10^5 cells/well. A total of 480 wells was assessed for each condition. The calculated method of the fusion efficiency (%): the total number of colonies in 480 wells were counted, then divided by the number of input B cells and multiplied by 100. The columns represent the average fusion efficiency (%) of 3 experiments, the error bars represent the SD.

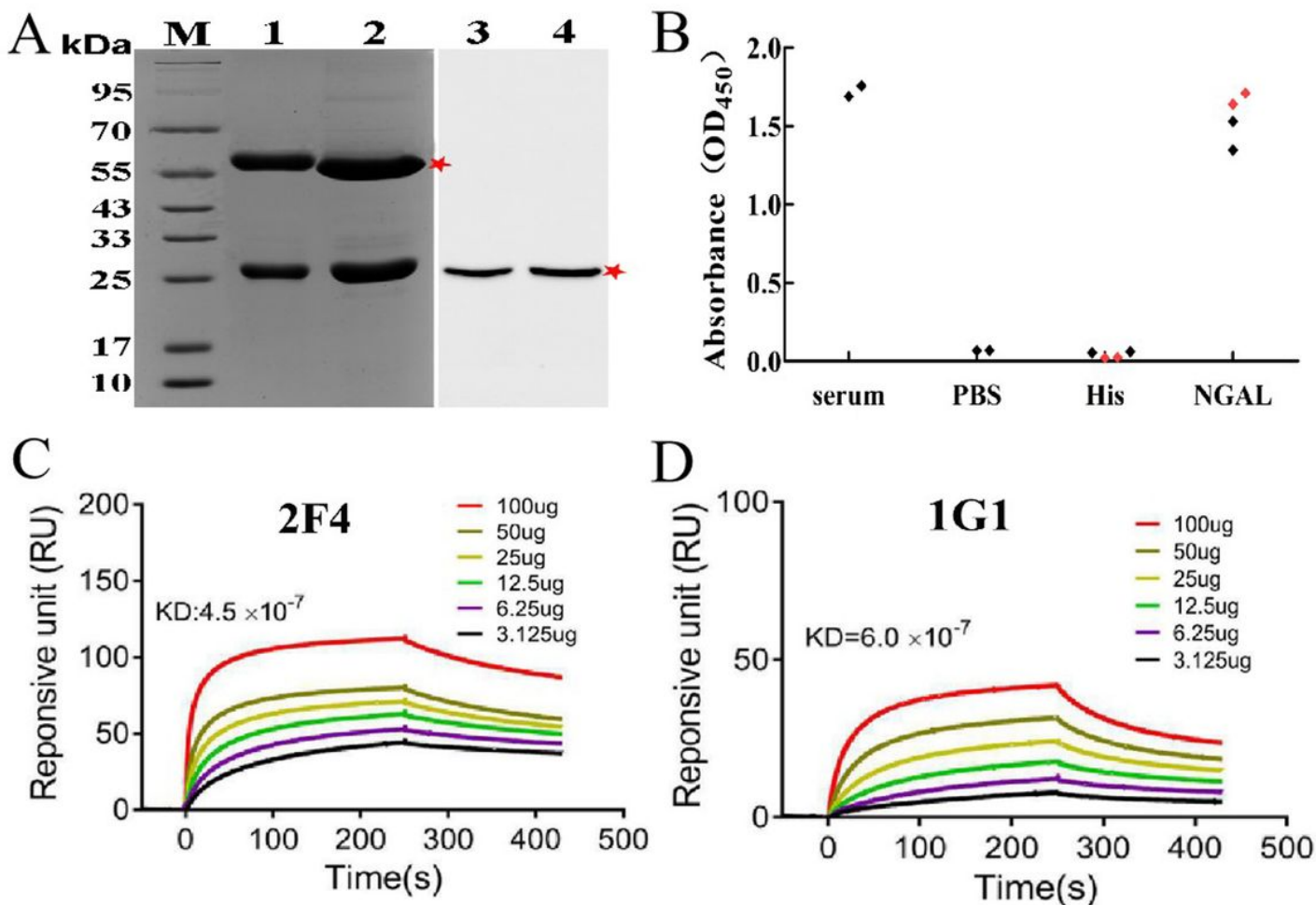


Figure 3

Characterization of monoclonal antibodies. (A) The ascites were assessed by SDS-PAGE and Western blot, Lane M, protein marker; Lane 1, purified the ascites of 2F4; Lane 2, purified the ascites of 1G1; Lane 3, Western blot analysis of mAb 2F4 ; Lane 4, Western blot analysis of mAb 1G1. (B) The Cross-reactivity of 2 hybridoma lines was tested by Indirect ELISA, NGAL-6×His and PCT-6×His were coated onto microtiter plates. The positive control was a NGAL-6×His immune serum; PBS were used as blank control. (C) Relative affinity of MAb 2F4. (D) Relative affinity of MAb 1G1.

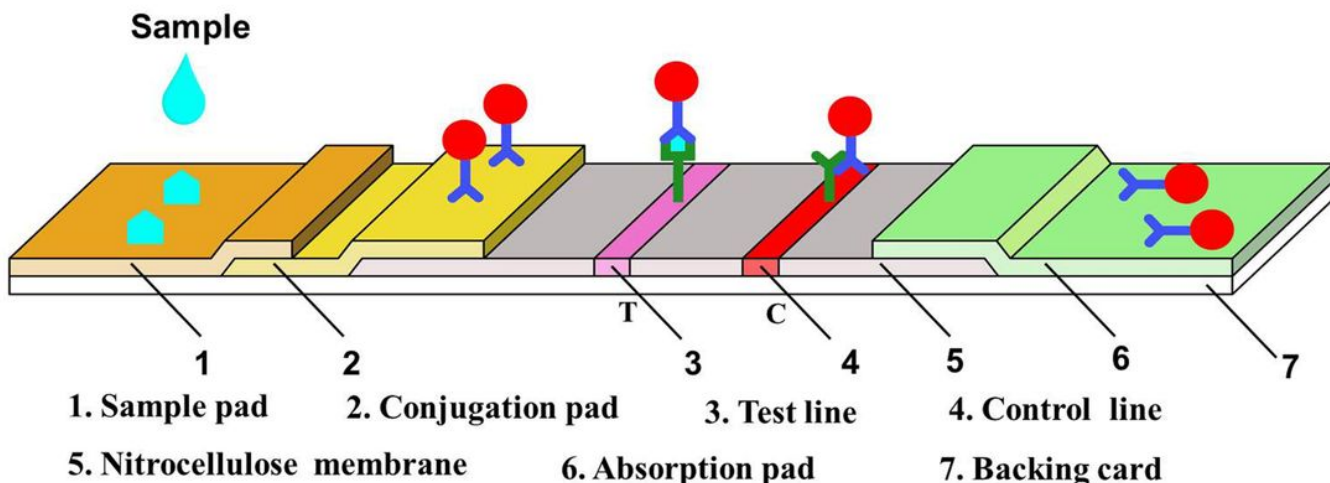


Figure 4

Schematic description of fluorescence immunoassay system employed Europium-conjugated NGAL mAbs.

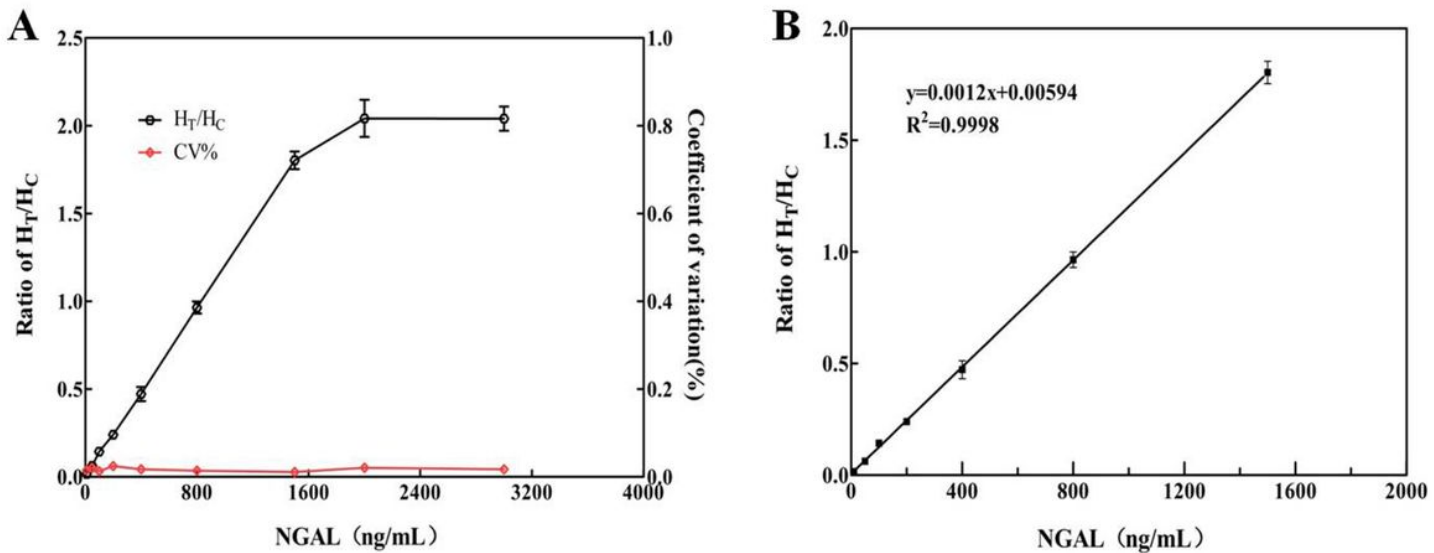


Figure 5

Standard curves for NGAL. (A) The ratio of HT/HC, by antibody pairing in LFIA, the antibody pairs 2F4-labeled1G1 ratio of HT/HC rose with increasing concentration of NGAL. (B) The standard curve of NGAL.

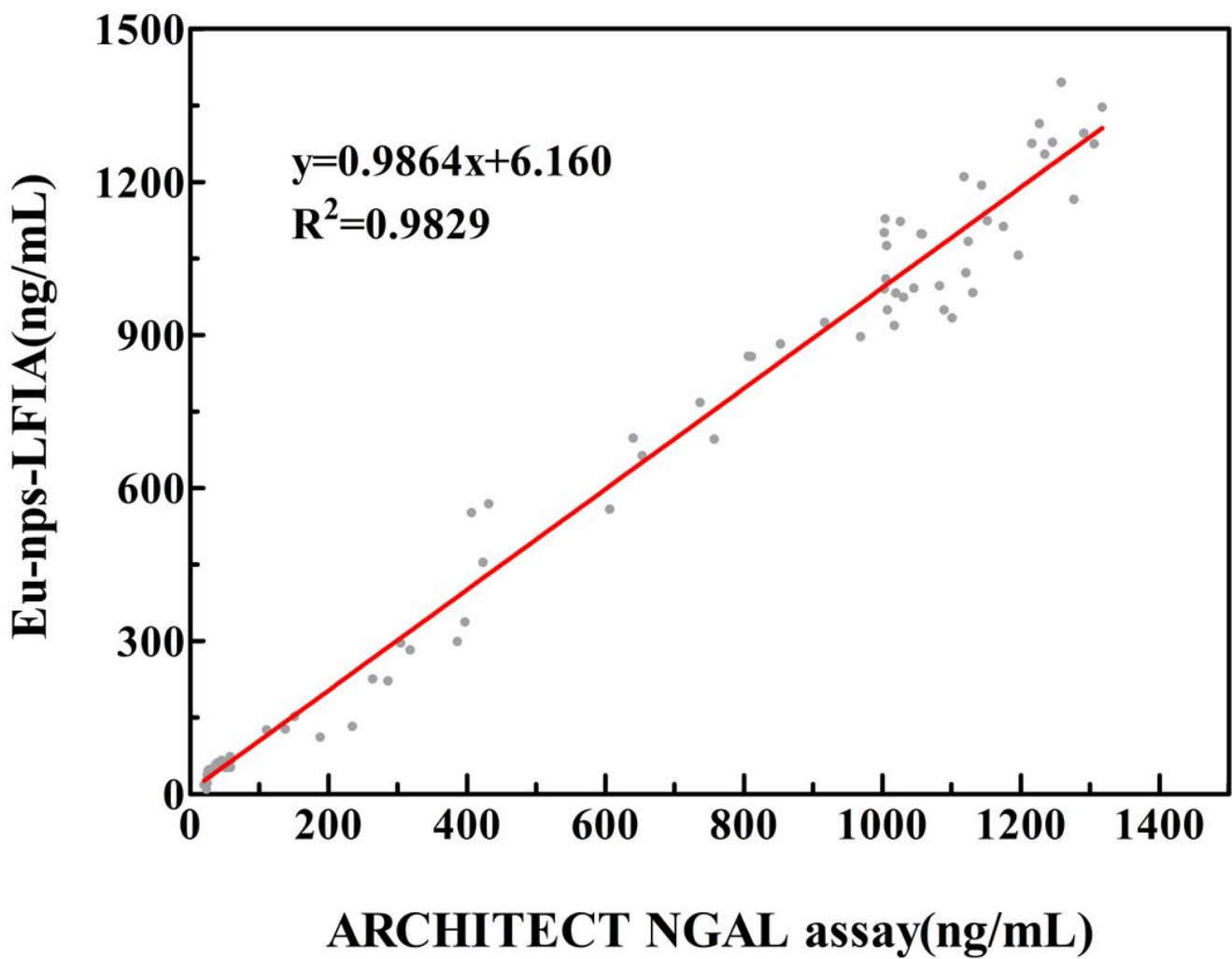


Figure 6

Comparison of EU-NPS-LFIA with ARCHITECT urine assay estimated correlation of the results for NGAL clinical test.